

Highly efficient exchange of orbital angular momentum of light via electron spin coherence

Omar A Alkawak¹, Al-Behadili Faisal Raheem², Yaser Yasin³,
Wessim Salahaddin Ibrahim⁴, Ali Abdul Kadhim Ruhaima⁵, Zahraa Hassan Ward⁶,
Salema K Hadrawi^{7,8} and H Kong^{7,9,*}

¹ Air conditioning and Refrigeration Techniques Engineering Department, Al-Mustaqbal University College, Babylon, Iraq

² University of Ahl Al Bayt, Kerbala, Iraq

³ College of Medical Technology, Al-Farahidi University, Baghdad, Iraq

⁴ Department of Dentistry, AlNoor University College, Bartella, Iraq

⁵ AL-Nisour University College, Baghdad, Iraq

⁶ Mazaya University College, Nasiriyah, Iraq

⁷ Refrigeration and Air-conditioning Technical Engineering Department, College of Technical Engineering, The Islamic University, Najaf, Iraq

⁸ Computer Engineering Department, Imam Reza University, Mashhad, Iran

⁹ Department of optoelectronic and quantum technology, Henan Institute of Technology, Xinxiang Henan 453003, People's Republic of China

E-mail: huijunkong126@gmail.com

Received 20 October 2022

Accepted for publication 30 October 2022

Published 30 November 2022



Abstract

In this letter we analysed the efficient exchange of orbital angular momentum (OAM) of light in a double V-type semiconductor quantum well via electron spin coherence. We found that due to the four-wave mixing (FWM) mechanism the OAM state of the vortex light can transfer from applied lights to a new generated signal beam when the efficiency of the FWM processes is enough high. We also shown that the absorption spectrum of the new generated light depends on the OAM number and azimuthal angle of the optical vortex light. We realized that for some specific parametric conditions the absorption spectrum of the generated light becomes negative which corresponds to the lasing without inversion.

Keywords: orbital angular momentum, electron spin coherence, exchange efficiency

(Some figures may appear in colour only in the online journal)

1. Introduction

It is well known that the main conditions for the observations of exciting phenomena like electromagnetically induced transparency (EIT) [1], optical bistability (OB) [2, 3], coherent population trapping [4, 5], optical solitons [6, 7], four-wave mixing (FWM) [8, 9], and others [10–16] are quantum coherence

and interference. In atomic systems [17, 18] or semiconductor quantum wells (QWs) [19, 20] and quantum dots [21, 22], these phenomena have been thoroughly researched. There has been extensive research on the function of electron spin coherence (ESC) in QWs [23–26]. Asadpour *et al* [26], for instance, have studied the OB properties of propagated light in a unidirectional ring cavity with QWs via the ESC effect. Experimental research on the optical control of ESC using linearly or circularly polarized laser beams has been done by Feng *et al* [27].

* Author to whom any correspondence should be addressed.

The interaction of optical vortex light carrying orbital angular momentum (OAM) with the atomic system has recently been observed [28–35]. An optical vortex is a beam that has an optical phase that depends on the azimuthal coordinate and a wavefront that is helical. OAM also gives a photon an extra degree of freedom, which makes it a higher-dimensional system for high-capacity information transfer. Recent research has shown that the coherent characteristics of EIT enable the identification of OAM information by generating spatially varying absorption patterns [31]. Through structure light and composite optical vortex light, the azimuthal dependence of the electromagnetically induced grating has been explored. It has been demonstrated that both symmetric and asymmetric diffraction patterns can be generated by adjusting the OAM number of the vortex light. A paradigm for producing new structure light through spatially dependent transparency using optical vortex light was put out by Qiu *et al* [36]. Mehdienejad [29] used optical vortex light to study the spatial regulation of atom-photon entanglement. It was discovered that altering the OAM number of the structure light can produce the highest degree of entanglement.

In this research, we suggested a new model for investigating the transfer of OAM state of light from optical vortex lights to a newly created signal beam based on ESC in QW waveguide. In recent years, numerous concepts have been put up for various architectures to exchange the OAM state of light [37–39].

2. Model and formulation

Consider a double V-type QW waveguide with ESC in figure 1. The corresponding system interacts with two control lights with Rabi frequencies $2\Omega_+$ and $2\Omega_2$. A weak probe field with Rabi frequency $2\Omega_-$ and a control light with Rabi frequency $2\Omega_2$ forms a first V-type scheme, while a weak generated signal beam with Rabi frequency $2\Omega_1$ and control field $2\Omega_+$ form the second V-type scheme, respectively. The more details about this scheme can be found in [25]. The Hamiltonian of the system can be given as follows:

$$H = \sum_{j=a,b,c,d} \varepsilon_j |j\rangle \langle j| - \hbar(\Omega_1 e^{-i\theta_1} |a\rangle \langle b| + \Omega_2 e^{-i\theta_2} |d\rangle \langle c| + h.c) - \hbar(\Omega_+ e^{-i\theta_+} |d\rangle \langle b| + \Omega_- e^{-i\theta_-} |a\rangle \langle c| + h.c) \quad (1)$$

where, ε_j corresponds to the energy of state $|j\rangle$, ($j = a, b, c, d$), $\theta_n = \omega_n t$, ($n = 1, 2, \pm$), ω_n show the frequencies of the applied lights. By using of $H_0 = \varepsilon_a |a\rangle \langle a| + (\varepsilon_a - \hbar\omega_1) |b\rangle \langle b| + (\varepsilon_a - \hbar\omega_-) |c\rangle \langle c| + (\varepsilon_a - \hbar\omega_- + \hbar\omega_1) |d\rangle \langle d|$ with $\varepsilon_a = 0$. We define the frequency of the FWM generated light as $\omega_1 = \omega_+ + \omega_- - \omega_2$. The Hamiltonian of the system in the interaction picture can be given as follow:

$$H_{int}/\hbar = \Delta_1 |b\rangle \langle b| + \Delta_- |c\rangle \langle c| + (\Delta_- - \Delta_2) |d\rangle \langle d| - (\Omega_1 |a\rangle \langle b| + \Omega_2 |d\rangle \langle c| + h.c) - (\Omega_+ |d\rangle \langle b| + \Omega_- |a\rangle \langle c| + h.c) \quad (2)$$

where $\Delta_1 = \omega_1 - \omega_{ab}$, $\Delta_+ = \omega_+ - \omega_{db}$, $\Delta_- = \omega_- - \omega_{ac}$, $\Delta_2 = \omega_2 - \omega_{dc}$ and $\omega_{jm} = (\varepsilon_j - \varepsilon_m)/\hbar$ ($j = a, b, c, d; j \neq m$) show the transition frequencies. By defining the state $|\psi\rangle = A_a |a\rangle + A_b |b\rangle + A_c |c\rangle + A_d |d\rangle$, the equations of motions can be given as follows:

$$\begin{aligned} i \frac{\partial}{\partial t} A_a &= -i\gamma_a A_a - \Omega_1 A_b - \Omega_- A_c, \\ i \frac{\partial}{\partial t} A_b &= (\Delta_1 - i\gamma_b) A_b - \Omega_1^* A_a - \Omega_+^* A_d, \\ i \frac{\partial}{\partial t} A_c &= (\Delta_- - i\gamma_c) A_c - \Omega_2^* A_d - \Omega_-^* A_a, \\ i \frac{\partial}{\partial t} A_d &= (\Delta_- - \Delta_2 - i\gamma_d) A_d - \Omega_2 A_c - \Omega_+ A_b, \end{aligned} \quad (3)$$

where γ_j ($j = a, b, c, d$) corresponds to the decay rates of the state j . By assuming that the system is initially in the electron state $|a\rangle$ ($A_a \simeq 1$) and $|\Omega_{2,+}| \gg |\Omega_{1,-}|$, we have:

$$(-\Delta_1 + i\gamma_b) A_b + \Omega_+^* A_d = -\Omega_1^* \quad (4a)$$

$$(-\Delta_- + i\gamma_c) A_c + \Omega_2^* A_d = -\Omega_-^* \quad (4b)$$

$$(\Delta_2 - \Delta_- + i\gamma_d) A_d + \Omega_2 A_c + \Omega_+ A_b = 0 \quad (4c)$$

The equation (4) can be solved analytically for obtaining the relation A_b and A_c as follows:

$$A_b^* = -\frac{H_p}{H} \Omega_1 - \frac{\Omega_2^* \Omega_+}{H} \Omega_- \quad (5a)$$

$$A_c^* = -\frac{\Omega_2 \Omega_+^*}{H} \Omega_1 + \frac{H_c}{H} \Omega_- \quad (5b)$$

where, we have:

$$H_p = |\Omega_2|^2 - (\Delta_- + i\gamma_c)(\Delta_2 - \Delta_- - i\gamma_d) \quad (6a)$$

$$H_c = |\Omega_+|^2 + (\Delta_1 + i\gamma_b)(\Delta_2 - \Delta_- - i\gamma_d) \quad (6b)$$

$$H = |\Omega_+|^2 (\Delta_- + i\gamma_c) + |\Omega_+|^2 (\Delta_1 + i\gamma_b) + (\Delta_1 + i\gamma_b)(\Delta_- + i\gamma_c)(\Delta_2 - \Delta_- - i\gamma_d) \quad (6c)$$

We consider the situation where all the waves propagate along z direction. Therefore, we have:

$$\frac{\partial}{\partial z} \Omega_1 = ik_{ab} A_b^* \quad (7a)$$

$$\frac{\partial}{\partial z} \Omega_- = ik_{ac} A_c^* \quad (7b)$$

where $k_{ab(ac)} = 2N\omega_{1(-)} |\mu_{ab(ac)}|^2 / \hbar c$. Parameter N shows the effective density and $\mu_{ab(ac)}$ corresponds to the dipole moment for the transition between states $|a\rangle$ and $|b\rangle$, $|c\rangle$. By substituting

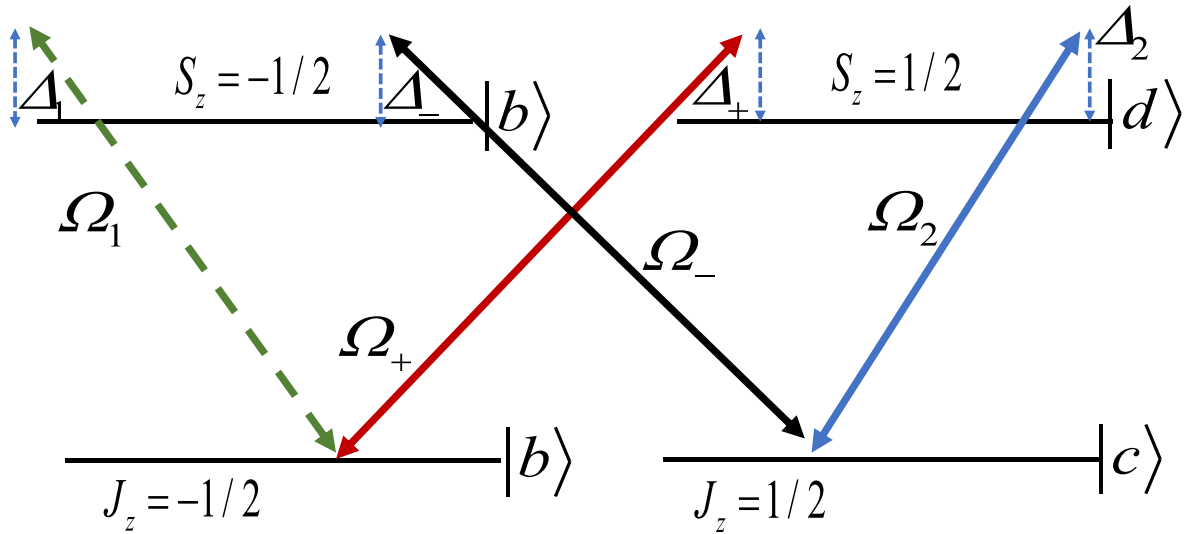


Figure 1. The configuration of double V-type quantum well waveguide where two upper electron spin coherence state couples to the ground levels.

the equation (5) in equation (7), and for $\Omega_-(z=0) = \Omega_-(0)$ and $\Omega_1(z=0) = 0$, we have:

$$\Omega_1(z) = -i\Omega_-(0) \frac{e^{izk_+} - e^{izk_-}}{W_+ - W_-} \quad (8a)$$

$$\Omega_-(z) = \Omega_-(0) \frac{W_+ e^{izk_+} - W_- e^{izk_-}}{W_+ - W_-} \quad (8b)$$

where

$$k_{\pm} = \frac{k_{ac}H_c - k_{ab}H_p \pm \sqrt{D}}{2H} \quad (9a)$$

$$W_{\pm} = \frac{k_{ac}H_c + k_{ab}H_p \pm \sqrt{D}}{2k_{ab}k_{ac}\Omega_2^*\Omega_+} \quad (9b)$$

$$D = (k_{ac}H_c + k_{ab}H_p)^2 + 4k_{ab}k_{ac}|\Omega_+|^2|\Omega_2|^2 \quad (9c)$$

The equation (8) are the main results of our paper and in the follow, we will investigate the exchange efficiency, transfer of optical vortex light and spatially dependent of the generated signal light in different conditions of the optical parameters.

3. Results and discussion

In the following, we will discuss exchange efficiency of the optical vortex of light via adjusting the optical parameters of the system. We will show that the transfer of the optical vortex is possible in different conditions of the medium. In figure 2, we show the exchange efficiency versus parameter Z/L for different intensity of the Rabi frequency Ω_2 . Here, we realized that by enhancing the Rabi frequency, the exchange

efficiency increases and for $\Omega_2 = 0.7\gamma$ (dotted line) reaches to its maximum value. In this case, due to absorption losses of the medium, the generated light slightly oscillates, but when propagates deeper through the medium, the absorption disappears, respectively. In figure 3, we display the exchange efficiency versus detuning of the generated light for different Rabi frequency Ω_2 . Here also we find that the exchange efficiency increases by enhancing the Rabi frequency of the coupling light. However, the exchange efficiency is slightly higher on the sides of the resonant condition of the generated light with its transition. This result has a good agreement with our previous result in figure 2. In the following, we assume that one or more of the vertex fields contain optical vorticities. The formulation the optical vortex light by Rabi frequency is given as follow:

$$\Omega_i = \varepsilon_i \left(\frac{r}{w}\right)^{|l_i|} e^{-r^2/w^2} e^{il_i\varphi} \quad (10)$$

where, the parameters ε_i , r , w , l_i and φ are defined as strength of the vortex light, the distance from the vortex core in cylindrical radius, beam waist, OAM number and azimuthal angle, respectively. In figure 4, we consider that the coupling light Ω_2 is optical vortex and plot the exchange efficiency versus parameter r/w for different optical vorticity. Here, one can find that the exchange efficiency is not high for small vortex values. But for its larger value i.e. $l_2 = 4$ (dashed-dotted line), a large jump in the efficiency value appears and reaches the maximum value. In fact, controlling the value of the vortex at different locations and phases leads to controlling the intensity of the coupling field, and this controls the efficiency at different points of the vortex beam. We know that due to the closed-loop configuration of our model, the azimuthal angle can affect the optical properties of the medium. Therefore,

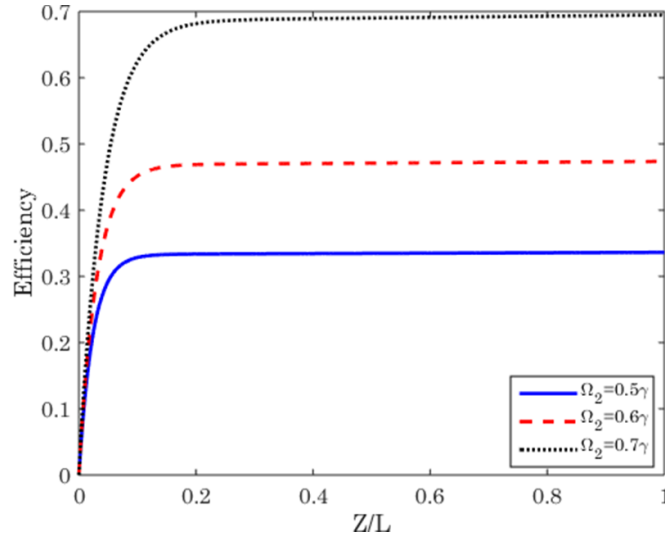


Figure 2. Efficiency of the generated signal beam versus propagation length for different values of Rabi frequency Ω_2 . The solid line corresponds to the $\Omega_2 = 0.5\gamma$, dashed line corresponds to the $\Omega_2 = 0.6\gamma$ and dotted line corresponds to the $\Omega_2 = 0.7\gamma$. The other selected parameters are $\Delta_{\pm} = \Delta_1 = \Delta_2 = 0$, $2\gamma_b = 2\gamma_c = \gamma$, $2\gamma_d = 2\gamma_a = 0.0001\gamma$, $\Omega_1 = \gamma$.

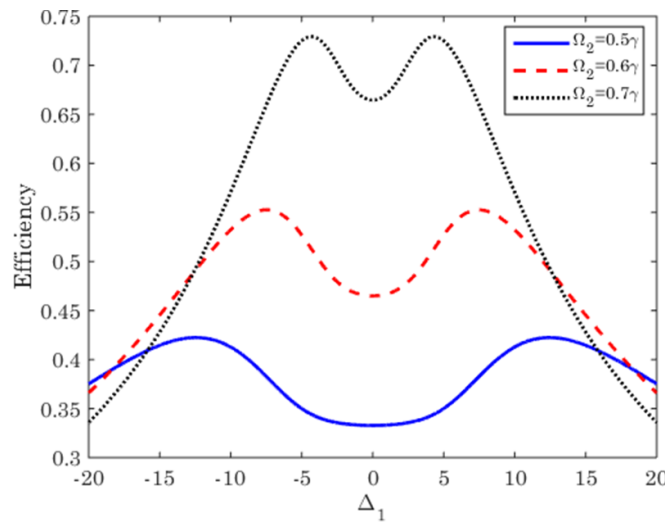


Figure 3. Exchange efficiency versus detuning of the generated light for different values of Rabi frequency Ω_2 . The solid line corresponds to the $\Omega_2 = 0.5\gamma$, dashed line corresponds to the $\Omega_2 = 0.6\gamma$ and dotted line corresponds to the $\Omega_2 = 0.7\gamma$. The other selected parameters are same as figure 2.

in figure 5, we plot the absorption (a) and dispersion (b) of the generated signal light versus its detuning for different azimuthal angle ϕ . It can be seen that the absorption and dispersion spectrums of the probe light depends strongly to the azimuthal angle of the vortex light. In this case, the probe light can be amplified by altering the azimuthal angle and simultaneously the slop of the dispersion can be changed from positive to negative, respectively. In figure 6, we display the absorption (a) and dispersion (b) properties versus detuning of the generated light for different propagation length. Here, we realize that the absorption of the generated light depends completely to the propagation length. Here, we find that at first, the generated field is absorbed and at the end, is amplified. Moreover, the slop of the dispersion is changed for different

values of propagation length. In figure 7, we show the intensity (a), (d) phase (b), (e) and absorption (c), (f) spectrums of the generated light for different OAM numbers of vortex light. It can be seen that for a small OAM number, the intensity of the generated light has small hole and for large OAM number, the intensity pattern has a large hole. Moreover, it can be seen that the phase and absorption of the generated light depends on the OAM number, respectively. The phase profile shows that the number of the cycles around the circumference depends to the OAM number. The absorption spectrum of the generated light changes periodically by adjusting the OAM number, respectively. Here, we realized that the gain and absorption region equal to the OAM number of the vortex light.

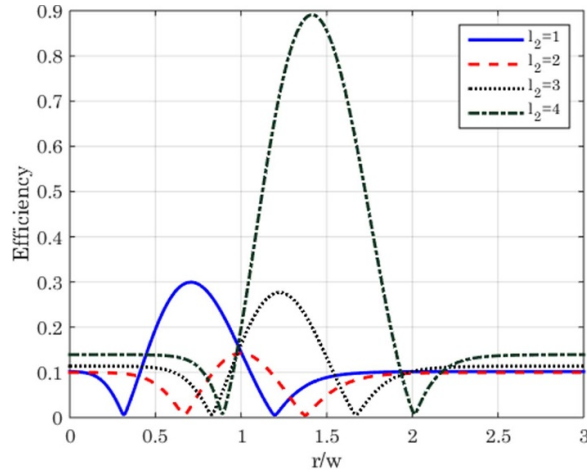


Figure 4. Exchange efficiency versus r/w for different OAM number of the vortex light. The solid line corresponds to the $l_2 = 1$, dashed line corresponds to $l_2 = 2$, dotted line corresponds to the $l_2 = 3$ and dashed-dotted line corresponds to $l_2 = 4$. The selected parameters are $Z = L$, $\varepsilon_2 = 3.5\gamma$, $\phi = \pi/2$ and others are same as figure 2.

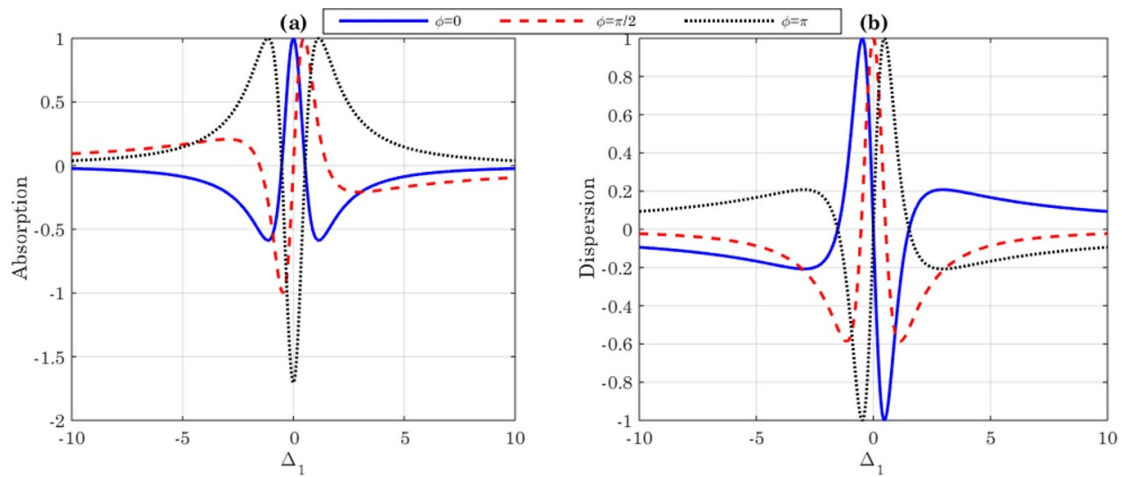


Figure 5. Absorption (a) and dispersion (b) spectrums versus detuning of the generated light for different azimuthal angle. The solid line corresponds to the $\phi = 0$, dashed line corresponds to $\phi = \pi/2$ and dotted line corresponds to $\phi = \pi$. The selected parameters are $r/w = 1$, $l_2 = 1$, $\varepsilon_2 = 3.5\gamma$, $Z = L$ and others are same as figure 2.

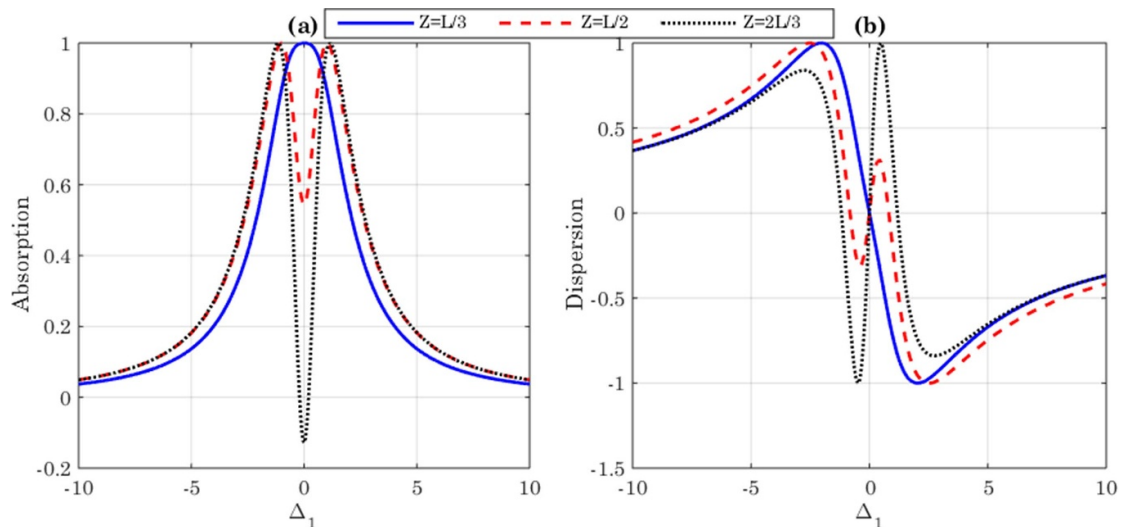


Figure 6. Absorption (a) and dispersion (b) spectrums versus detuning of the generated light for different propagation length. Solid line corresponds to $Z = L/3$, dashed line corresponds to $Z = L/2$ and dotted line corresponds to $Z = 2L/3$. The selected parameters are $l_2 = 1$, $\phi = \pi$ and others are same as figure 5.

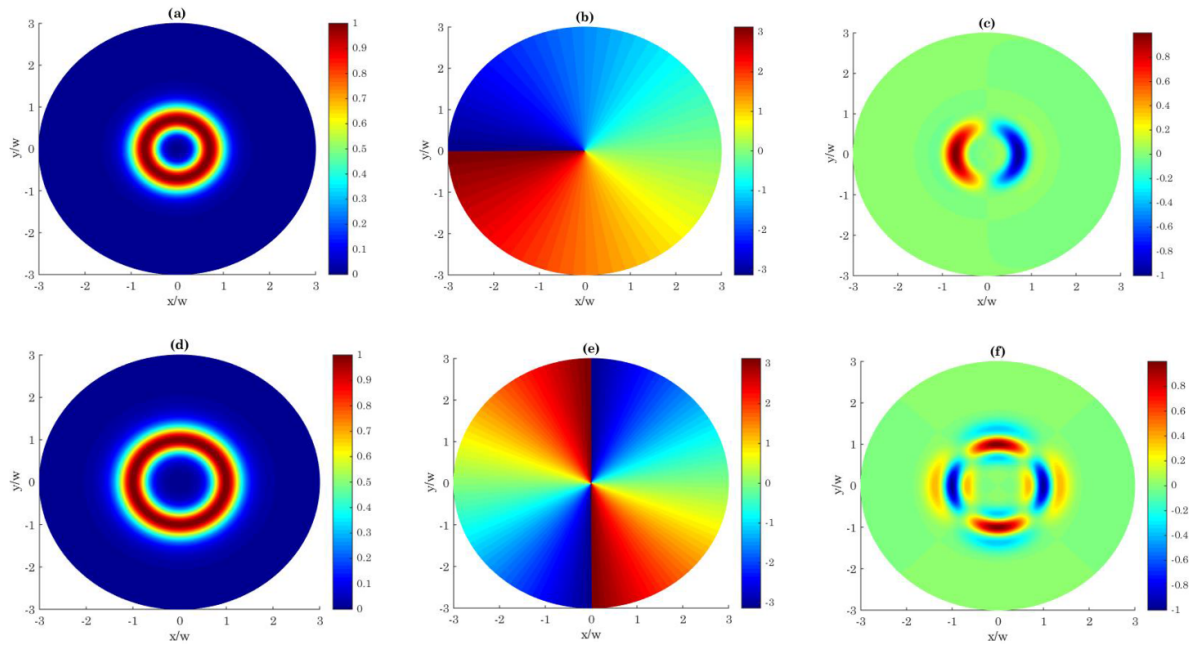


Figure 7. Intensity (a), (d) phase (b), (e) and absorption (c), (f) spectrums of the generated signal light versus normalized positions x/w and y/w for $l_2 = 1, 3$. The selected parameters are same as figure 2.

4. Conclusion

In summary, we have studied the exchange efficiency of the OAM via ESC in a double V-type QW nanostructure. Here, we assumed that the system prepared in ESC condition. Then, we study the generation of the FWM mechanism in the system analytically. We show that the exchange efficiency can be controlled by various parameters such as intensity of the coupling light and orbital angular momentum. Moreover, we discussed the absorption and dispersion profiles of the generated light for different values of azimuthal angle and propagation length. At the end, we studied the spatially distribution of the intensity, phase and absorption of the generated light for different winding number.

References

- [1] Wu Y and Yang X 2005 *Phys. Rev. A* **71** 053806
- [2] Solookinejad G, Jabbari M, Nafar M, Ahmadi E and Asadpour S 2018 *J. Appl. Phys.* **124** 063102
- [3] Solookinejad G, Jabbari M, Nafar M, Ahmadi Sangachin E and Asadpour S H 2019 *Int. J. Theor. Phys.* **58** 1359–68
- [4] Kirova T, Jia N, Asadpour S H, Qian J, Juzeliūnas G and Hamed H R 2020 *Opt. Lett.* **45** 5440–3
- [5] Hu X-M and Zhang J-P 2004 *J. Phys. B: At. Mol. Opt. Phys.* **37** 345–56
- [6] Wu Y and Deng L 2004 *Phys. Rev. Lett.* **93** 143904
- [7] Wu Y 2005 *Phys. Rev. A* **71** 053820
- [8] Wu Y and Yang X 2004 *Phys. Rev. A* **70** 053818
- [9] Wu Y and Yang X 2007 *Phys. Rev. B* **76** 054425
- [10] Wang Z, Zhen S and Yu B 2015 *Laser Phys. Lett.* **12** 046004
- [11] Song F, Wang Z, Juan R and Yu B 2019 *Appl. Phys. B* **125** 69
- [12] Xu X and Nieto-Vesperinas M 2019 *Phys. Rev. Lett.* **123** 233902
- [13] Asadpour SH 2018 *Optics Commun* **421** 125–33
- [14] Li Q, Cai X, Liu T, Jia M, Wu Q, Zhou H, Liu H, Wang Q, Ling X and Chen C 2022 *NanoPhotonics* **11** 2085–96
- [15] Asadpour SH, Hamed HR and Jafari M 2018 *Appl. Opt.* **57** 4013–9
- [16] Asadpour SH and RahimpourSoleimani XH 2014 *JOSA B* **31** 3123–30
- [17] Asadpour S H and Soleimani H R 2013 *Opt. Quantum Electron.* **46** 709–18
- [18] Hossein Asadpour S and Eslami-Majd A 2012 *J. Lumin.* **132** 1477–82
- [19] Asadpour S H and Soleimani H R 2014 *Physica B* **434** 112–7
- [20] Asadpour S H and Soleimani H R 2014 *Physica B* **449** 77–84
- [21] Peng Y, Yang A, Chen B, Zhang S, Liu S and Wang X 2016 *Laser Phys. Lett.* **13** 025401
- [22] Tian S-C, Wan R-G, Tong C-Z, Fu X-H, Cao J-S and Ning Y-Q 2015 *Laser Phys. Lett.* **12** 125203
- [23] Yang X-X, Li Z-W and Wu Y 2005 *Phys. Lett. A* **340** 320–5
- [24] Asadpour S H and Soleimani H R 2014 *Opt. Commun.* **315** 394–8
- [25] Liu J B, Liu N, Shan C J, Liu T K and Huang Y X 2010 *Phys. Rev. E* **81** 036607
- [26] Asadpour S H, Jaber M and Soleimani H R 2013 *J. Opt. Soc. Am. B* **30** 1815
- [27] Feng D H, Shan L F, Jia T Q, Pan X Q, Tong H F, Deng L, Sun Z R and Xu Z Z 2013 *Appl. Phys. Lett.* **102** 062408
- [28] Hamideh Kazemi S and Mahmoudi M 2019 *Laser Phys. Lett.* **16** 076001
- [29] Mehdinejad A 2022 *Int. J. Theor. Phys.* **61** 168
- [30] Asadpour S H, Hamed H R, Kirova T and Paspalakis E 2022 *Phys. Rev. A* **105** 043709
- [31] Hamed H R, Kudriasov V, Ruseckas J and Juzeliunas G 2018 *Opt. Express* **26** 28249–62
- [32] Rahmatullah M A and Ziauddin S Q 2020 *Phys. Rev. A* **101** 023821
- [33] Amini Sabegh Z, Maleki M A and Mahmoudi M 2019 *Sci. Rep.* **9** 3519

- [34] Hamed H R, Paspalakis E, Žlabys G, Juzeliūnas G and Ruseckas J 2019 *Phys. Rev. A* **100** 023811
- [35] Asadpour S H, Kirova T, Qian J, Hamed H R, Juzeliūnas G and Paspalakis E 2021 *Sci. Rep.* **11** 1–11
- [36] Qiu J, Wang Z and Yu B 2019 *Quantum Inf. Process.* **18** 160
- [37] Asadpour S H, Faizabadi E, Kudriašov V, Paspalakis E and Hamed H 2021 *Eur. Phys. J. Plus* **136** 1–13
- [38] Asadpour S H, Abbas M and Hamed H R 2022 *Phys. Rev. A* **105** 033709
- [39] Asadpour S H, Paspalakis E and Hamed H R 2021 *Phys. Rev. A* **103** 063705